

# Polarization filter based on linear Radon transform and elliptical elements to extract surface waves in 3C seismic data

Ivan J. Sánchez-Galvis\*, William Agudelo†, Daniel O. Trad‡ and Daniel Sierra\*,

## ABSTRACT

Polarization filters are an alternative tool to attenuate ground roll when multicomponent seismic data are available. These filters can separate surface and body waves by discriminating elliptical from linear motions. Existing polarization filters work in single-station. Thus, they can filter seismic data with irregular spatial sampling. However, in most cases, polarization filters do not get results similar to  $f - k$  filters because they do not operate in multitrace, and there is no velocity discrimination. We present a new polarization filter to extract surface waves from multitrace 3C seismic data. The filter works in the frequency-slowness domain as a mask on elliptic elements obtained from the linear Radon model of the seismic data in the frequency domain. We applied this filter on a 3C real shot gather from land seismic data acquired in the Middle Magdalena Valley in Colombia. The results show that this polarization filter can accurately extract the surface waves, preserving more low-frequency energy than the  $f - k$  filter.

## INTRODUCTION

Surface wave extraction is a crucial stage in the signal processing workflow in seismic exploration. Surface waves, also named ground roll, are considered coherent noise that masks the information of body wave reflections from deeper structures. Predominantly, surface waves are composed of Rayleigh waves, which are elliptically polarized waves that propagate with lower frequency and velocity than reflected waves. Therefore, filter design should use all these characteristics to extract surface waves in seismic shot gathers.

Filters in the  $f - k$  domain are commonly used to separate surface waves and body wave reflections by exploiting their differences in frequency and wavenumber (Yilmaz, 2001). However,  $f - k$  filters require regularly sampled data in time and space. But, this is rarely sometimes the case for land seismic exploration. One alternative to address this limitation is the linear Radon transform (LRT) in the frequency domain, which maps a model from the frequency-slowness into the data space in the frequency-offset. LRT filters can accurately extract surface waves (Luo et al. 2009; Hu et al. 2016).

Nevertheless,  $f - k$  and LRT filters fail when the energy of surface and body waves overlap in frequency and velocity. In the case of multicomponent data, another alternative is using polarization filters to extract surface waves (Kendall et al. 2005; Pinnegar 2006; Sánchez-Galvis et al. 2016). These filters can separate elliptically and linearly polarized events in a single-station. However, multitrace information (such as velocity) is not used. We present a new polarization filter that extracts elliptically polarized events in the

---

\*Universidad Industrial de Santander

†Centro de Innovación y Tecnología - ECOPEPETROL S.A.

‡CREWES - University of Calgary

frequency-slowness domain. The filter works as a mask over elliptic elements obtained from the linear Radon model of the seismic data in the frequency domain. We applied the filter on a 3C shot gather from field data acquired in the Middle Magdalena Valley in Colombia. The results show that the filter can accurately extract surface waves, including backscattering.

### ELLIPTICAL ELEMENTS OF 3C SEISMIC DATA

3C seismic traces can be represented by  $\mathbf{d}(t) = \{x(t), y(t), z(t)\}$ , where  $x(t)$ ,  $y(t)$  and  $z(t)$  are the radial, transverse and vertical data components, respectively. The 3C seismic trace can also be represented in the frequency domain by  $\mathbf{d}(f) = \{x(f), y(f), z(f)\}$  via the Fourier transform of every single component. For any particular frequency  $f$ , the 3C seismic trace can be decomposed by elliptical elements in the three-dimensional space:

$$\mathbf{d}(f) = Q \{a(f), b(f), I(f), \Omega(f), \omega(f), \phi(f)\} \quad (1)$$

where  $a$  is the semi-major axis of the ellipse,  $b$  is the semi-minor axis of the ellipse,  $I$  is the inclination angle,  $\Omega$  is the longitude of ascending node,  $\omega$  is the argument of pericentre, and  $\phi$  the phase respect to the time of maximum displacement. Figure 1 shows the geometry of a 3D elliptical motion described by the elliptical elements. The operator  $Q$  is the forward expression to get the spectra of the 3C seismic signal in terms of the spectra of elliptical elements. Likewise, the spectra of elliptical elements are obtained in terms of the spectra of 3C seismic signal by using the inversion expression:

$$\{a(f), b(f), I(f), \Omega(f), \omega(f), \phi(f)\} = Q^{-1} \{\mathbf{d}(f)\} \quad (2)$$

The derivation of the forward and inversion expressions are found in (Pinnegar 2006).

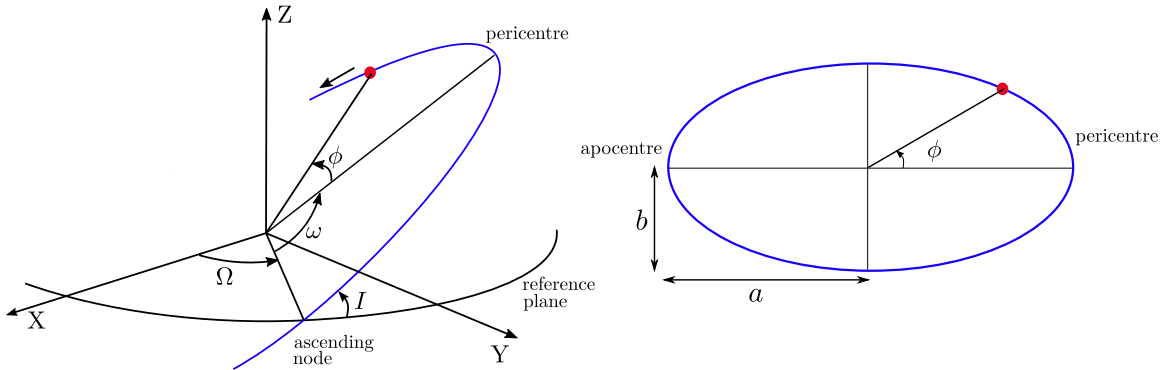


FIG. 1. Geometry of the 3D elliptical motion of a particle with semi-major axis  $a$ , semi-minor axis  $b$ , inclination angle  $I$ , longitude of ascending node  $\Omega$ , argument of pericentre  $\omega$ , and phase  $\phi$ .

For each shot gather, the 3C seismic data can be represented as a vectorial field  $\mathbf{d}(t, h)$  in the time-offset domain. After a temporal Fourier transformation, every single component of the 3C data can be mapped from the linear Radon model  $m(f, p)$  in the frequency-slowness domain by using the forward LRT in the frequency domain as follows:

$$d(f, h) = \sum_{p=p_{\min}}^{p_{\max}} m(f, p) e^{i2\pi f p h} \quad (3)$$

where  $p$  is the slowness.

The Radon model that best fits the data can be found by using an inversion scheme with sparsity constraint (Trad et al. 2003 Luo et al. 2009). The Radon model for 3C data can be represented by  $\mathbf{m}(f, p) = \{m_x(f, p), m_y(f, p), m_z(f, p)\}$  where  $m_x$ ,  $m_y$  and  $m_z$  are the Radon models for the radial, transverse and vertical data components, respectively. The elliptical elements can now be obtained in the frequency-slowness domain by substituting  $\mathbf{m}(f, p)$  in place of  $\mathbf{d}(f)$  in equation 2:

$$\{a(f, p), b(f, p), I(f, p), \Omega(f, p), \omega(f, p), \phi(f, p)\} = Q^{-1} \{\mathbf{m}(f, p)\} \quad (4)$$

### POLARIZATION FILTER

The 3C seismic data  $\mathbf{d}(t, h)$  can be expressed as a sum of surface waves  $\mathbf{d}^{\text{SW}}(t, h)$  and body waves  $\mathbf{d}^{\text{BW}}(t, h)$

$$\mathbf{d}(t, h) = \mathbf{d}^{\text{BW}}(t, h) + \mathbf{d}^{\text{SW}}(t, h) \quad (5)$$

By applying frequency domain adjoint LRT on both sides, the equation 5 becomes:

$$\mathbf{m}(f, p) = \mathbf{m}^{\text{BW}}(f, p) + \mathbf{m}^{\text{SW}}(f, p) \quad (6)$$

where  $\mathbf{m}^{\text{BW}}(f, p)$  and  $\mathbf{m}^{\text{SW}}(f, p)$  are the Radon models of the surface waves and body waves in the 3C seismic data, respectively.

The 3C surface waves radon model  $\hat{\mathbf{m}}^{\text{SW}}(f, p)$  is estimated by applying a filter mask in the semi-major and semi-minor of the decomposition of the elliptical elements. By omitting the arguments  $(f, p)$ , we have:

$$\hat{\mathbf{m}}^{\text{SW}} = Q(aF, bF, I, \Omega, \omega, \phi) \quad (7)$$

where  $F$  is the filter mask in the frequency-slowness domain. This filter mask is constructed by the activations functions  $F_f$ ,  $F_p$ , and  $F_b$  as follows:

$$F(f, p) = F_f(f)F_p(p)F_b(b(f, p)) \quad (8)$$

The definitions of the activation functions are:

$$F_f(f) = \frac{1}{2} + \frac{1}{2} \tanh(\alpha_f(f - f_{\text{ref}})), \quad (9)$$

$$F_p(p) = \frac{1}{2} - \frac{1}{2} \tanh(\alpha_p(|p| - p_{\text{ref}})) \quad (10)$$

$$F_b(b(f, p)) = \tanh\left(\alpha_b \frac{b(f, p)}{b_{\text{max}}}\right) \quad (11)$$

where  $b_{\text{max}}$  is the maximum value of  $b(f, p)$ , the parameters  $p_{\text{ref}}$  and  $f_{\text{ref}}$  are reference values to limit the operation zone of the filter in the slowness and frequency axis, respectively. The reference slowness value can be set by using the relation  $p_{\text{ref}} = 1/v_{\text{max}}$ , where  $v_{\text{max}}$  is the maximum surface waves velocity. Finally,  $\alpha_f$ ,  $\alpha_p$ , and  $\alpha_b$  are positive parameters that control the width of the transition zone of the activation functions. Figure 2 shows the behaviour of each activation function.

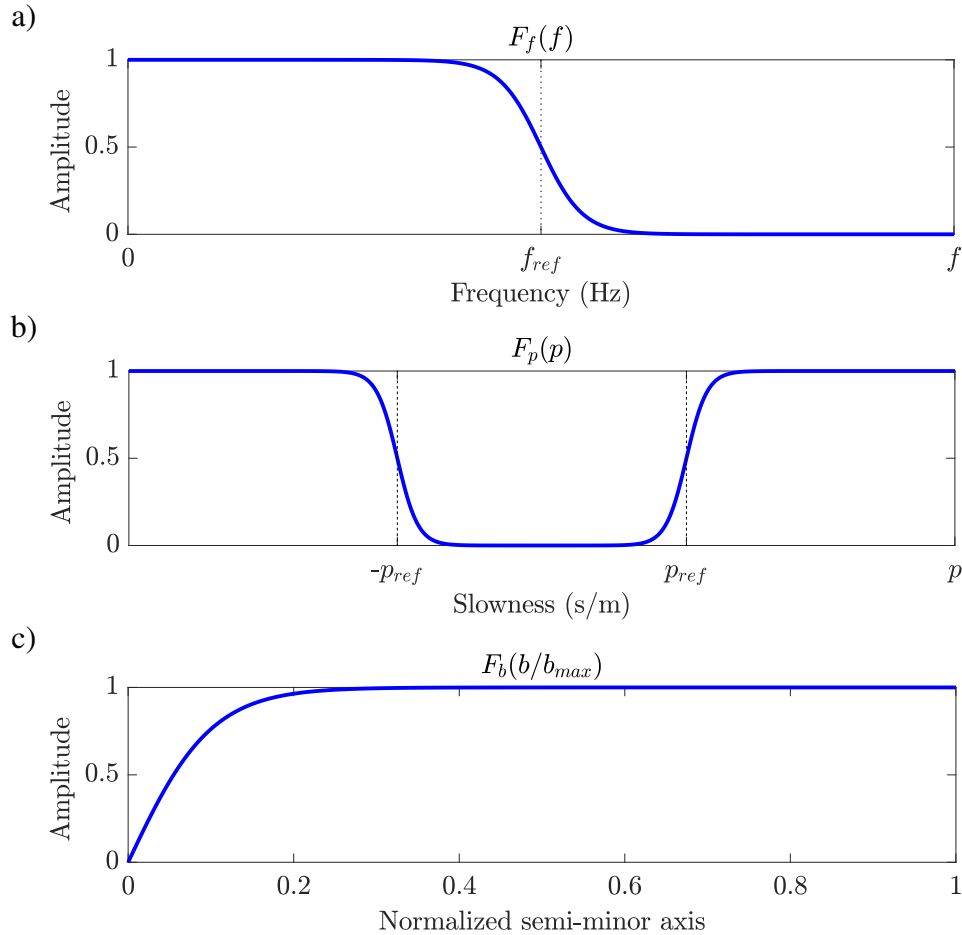


FIG. 2. Activation functions used to construct the polarization filter mask. a) Activation function for frequency. b) Activation function for slowness. c) Activation function for normalized semi-minor axis.

The extracted 3C surface waves  $\hat{\mathbf{d}}^{\text{SW}}(t, h)$  are obtained by the forward LRT of  $\hat{\mathbf{m}}^{\text{SW}}(f, p)$  and, subsequently applying the temporal inverse Fourier transform. Finally, the 3C body

waves  $\hat{\mathbf{d}}^{BW}(t, h)$  are obtained by the difference between the raw data and the extracted surface waves.

$$\hat{\mathbf{d}}^{BW}(t, h) = \mathbf{d}(t, h) - \hat{\mathbf{d}}^{SW}(t, h) \quad (12)$$

## RESULTS

We tested the proposed polarization filter on a 3C shot gather from seismic data acquired in the Middle Magdalena Valley in Colombia. The shot gather for the vertical, radial, and transverse components after a gain correction of  $t^2$  are displayed in Figure 5a. We observed that ground roll is considerably more complex for short offset than long offset. We interpret that the low-velocity and heterogeneous near-surface close to the source location produces backscattering and reverberations that mask the body wave reflections from deeper structures.

Figure 3 show the Radon panel of each elliptical element obtained from the raw data. In Figures 3a and 3b, which correspond to semi-major  $a(f, p)$  and semi-minor axis  $b(f, p)$ , respectively; we can identify the fundamental mode of the Rayleigh wave around  $p = 0.005$  (s/m). Higher modes of Rayleigh waves are present even since approximately  $p = 0.001$  (s/m). We also observe that most Radon model energy is scattered and bounded below 11 Hz. The information in the negative values of  $p$  correspond to linear events of the shot gather with negative slopes, which can be related to backscattered waves.

We compared the performance of the polarization filter with the  $f - k$  filter. The  $f - k$  filter is a dip mask with four parameters ( $v_1$ ,  $v_2$ ,  $v_3$ , and  $v_4$ ) that specify the attenuation range. The range between  $v_2$  and  $v_3$  is preserved, and the range below  $v_1$  or above  $v_4$  is attenuated. Figure 4a shows the  $f - k$  filter mask that we use to attenuate ground roll with  $v_1 = 100$  (m/s),  $v_2 = 200$  (m/s),  $v_3 = 600$  (m/s), and  $v_4 = 1000$  (m/s). On the other hand, The proposed polarization filter is a mask in the frequency-slowness domain that preserves the surface wave energy. Thus, the body wave energy is reconstructed by subtracting the extracted surface waves. According to the analysis performed for the ground roll of these seismic data, we set  $f_{\text{ref}} = 10$  Hz,  $p_{\text{ref}} = 1/750$  s/m. We tested different aggressiveness values, and we got the best results with  $\alpha_f = 1$ ,  $\alpha_p = 10^4$ , and  $\alpha_b = 12$ . Figure 4b shows the polarization filter mask used to extract the ground roll. The filtered data are obtained by subtracting the extracted ground roll from the raw data, as we showed in equation 12.

Figure 5b and 5c show the multicomponent shot gathers after  $f - k$  filtering and polarization filter, respectively. We observe minor differences between the resulting shot gathers of the  $f - k$  filter and the results of the polarization filter. Therefore, we also compared the results of these filters in the transformed domain. Figure 6 shows the  $f - k$  spectra of the multicomponent shot gather for the raw data, filtered data with  $f - k$  filter, and filtered data with the proposed polarization filter. We note that the polarization filter preserves more energy than the  $f - k$  filter in the attenuation range. Finally, we compared the Fourier spectra of the filtered data to evaluate the aggressiveness of each filter in the frequency domain. Figure 7 shows the spectra for the vertical, radial, and transverse components. The black line is the raw data; the filtered data is blue for the  $f - k$  filter and red for the polarization

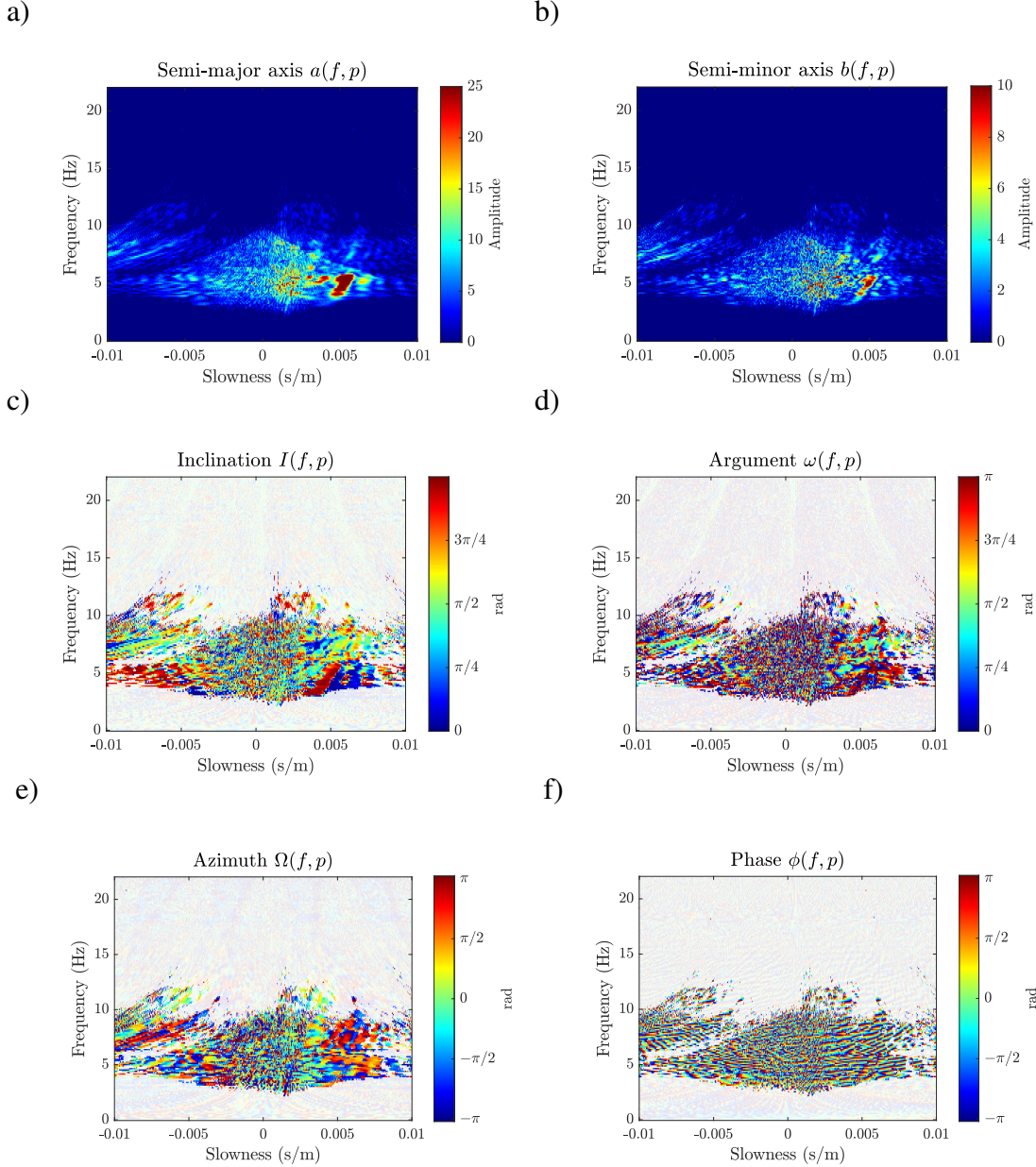


FIG. 3. Radon panels of elliptical elements computed from raw data in Figure 5a. (a) Semi-major axis  $a(f, p)$ , (b) semi-minor axis  $b(f, p)$ , (c) inclination  $I(f, p)$ , (d) argument of pericentre  $\omega(f, p)$ , (e) azimuth of ascending node  $\Omega(f, p)$ , and (f) phase  $\phi(f, p)$ .

filter. We can see that the polarization filter preserves more low-frequency energy than the  $f - k$  filter. This energy is related to low-frequency components of reflections since the polarization filter is designed to maintain linear polarization and attenuate elliptical polarization motions.

## CONCLUSIONS

We have presented a polarization filter to extract surface waves from 3C seismic data. The filter operates in the frequency-slowness domain as a mask on elliptic elements obtained from the linear Radon model of the seismic data in the frequency domain. This

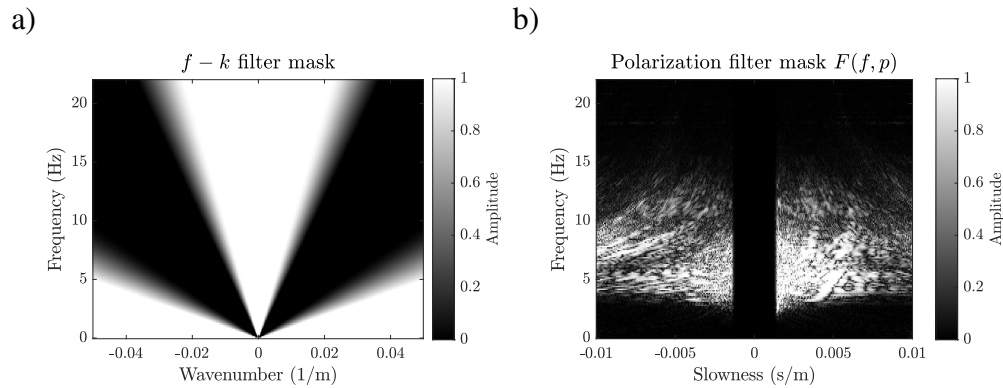


FIG. 4. (a)  $f - k$  filter mask with  $v_1 = 100$  (m/s),  $v_2 = 200$  (m/s),  $v_3 = 600$  (m/s), and  $v_4 = 1000$  (m/s). (b) Polarization filter mask  $F(f, p)$  with  $f_{\text{ref}} = 10$  Hz,  $p_{\text{ref}} = 1/750$  s/m,  $\alpha_f = 1$ ,  $\alpha_p = 10^4$ , and  $\alpha_b = 12$ .

filter differs from existing polarization filters because it takes into account the three variables that model ground roll (frequency, velocity, and polarization) while existing filters normally take into account two of them (frequency and polarization). The results obtained with real data show that this polarization filter can extract the surface waves and clean the body-waves reflections. Compared to  $f - k$  filter, the proposed polarization filter does allow to preserve low-frequency energy that is useful for the estimation of velocity models in seismic inversion. In this work, we only used the semi-minor axis to design the filter mask. However, additional elliptical elements can be included in tailored filters for different events, for instance, events with a specific incidence angle such as scattered surface waves.

## REFERENCES

- Hu, Y., Wang, L., Cheng, F., Luo, Y., Shen, C., and Mi, B., 2016, Ground-roll noise extraction and suppression using high-resolution linear radon transform: *Journal of Applied Geophysics*, **128**, 8–17.
- Kendall, R., Jin, S., Ronen, S., and De Meersman, K., 2005, An svd-polarization filter for ground roll attenuation on multicomponent data, *in* SEG Technical Program Expanded Abstracts 2005, Society of Exploration Geophysicists, 928–931.
- Luo, Y., Xia, J., Miller, R. D., Xu, Y., Liu, J., and Liu, Q., 2009, Rayleigh-wave mode separation by high-resolution linear radon transform: *Geophysical Journal International*, **179**, No. 1, 254–264.
- Pinnegar, C., 2006, Polarization analysis and polarization filtering of three-component signals with the time–frequency s transform: *Geophysical Journal International*, **165**, No. 2, 596–606.
- Sánchez-Galvis, I.-J., Serrano-Luna, J.-O., Niño-Niño, C.-A., Sierra, D.-A., and Agudelo-Zambrano, W.-M., 2016, Svd polarization filter taking into account the planarity of ground roll energy: *CT&F-Ciencia, Tecnología y Futuro*, **6**, No. 3, 5–24.
- Trad, D., Ulrych, T., and Sacchi, M., 2003, Latest views of the sparse radon transform: *Geophysics*, **68**, No. 1, 386–399.
- Yilmaz, Ö., 2001, *Seismic data analysis: Processing, inversion, and interpretation of seismic data*: Society of exploration geophysicists.

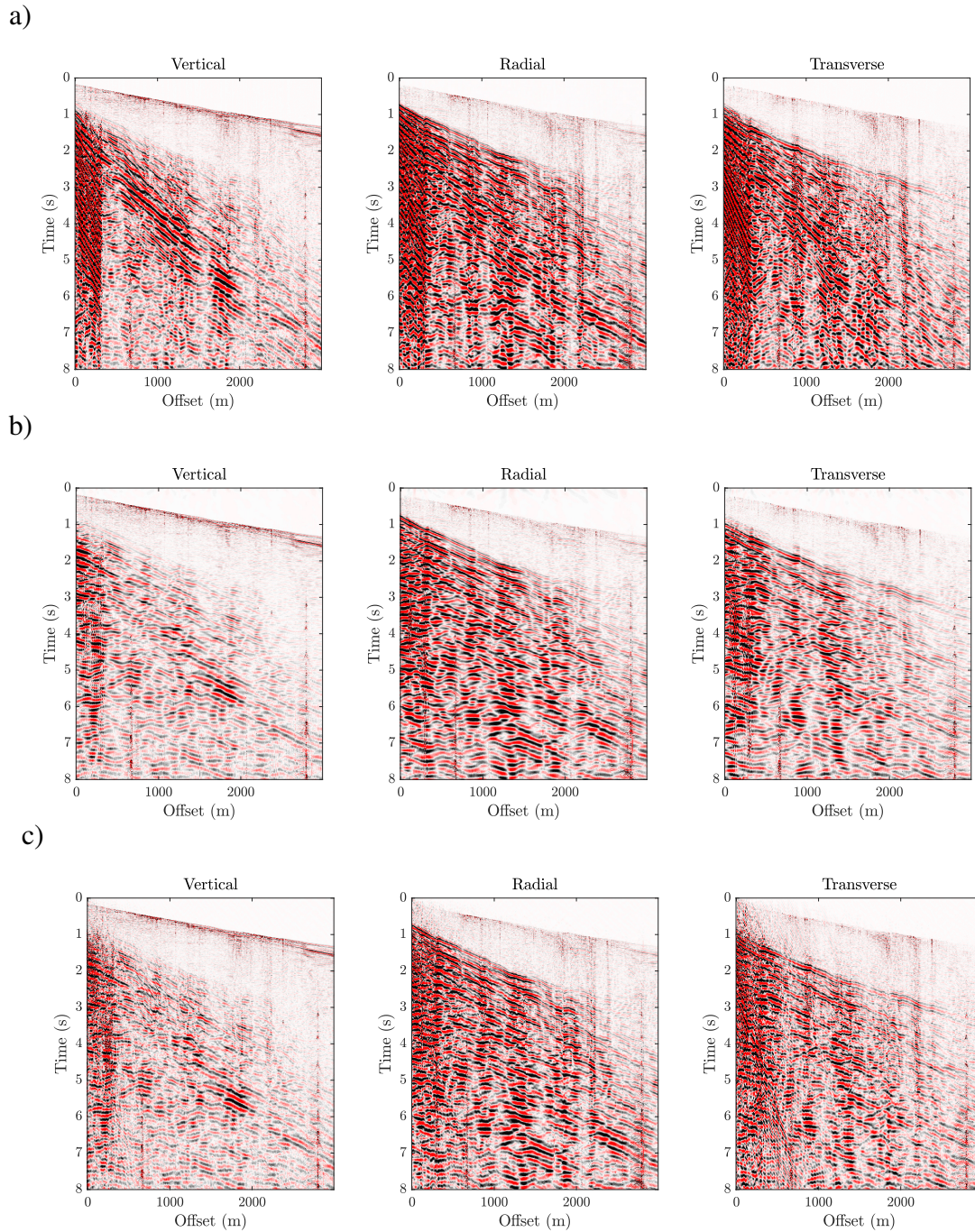


FIG. 5. Multicomponent shot gather of (a) raw data after a gain correction of  $t^2$ , (b) filtered data with the  $f - k$  filter, and (c) filtered data with the 3C polarization filter based in Radon transform.

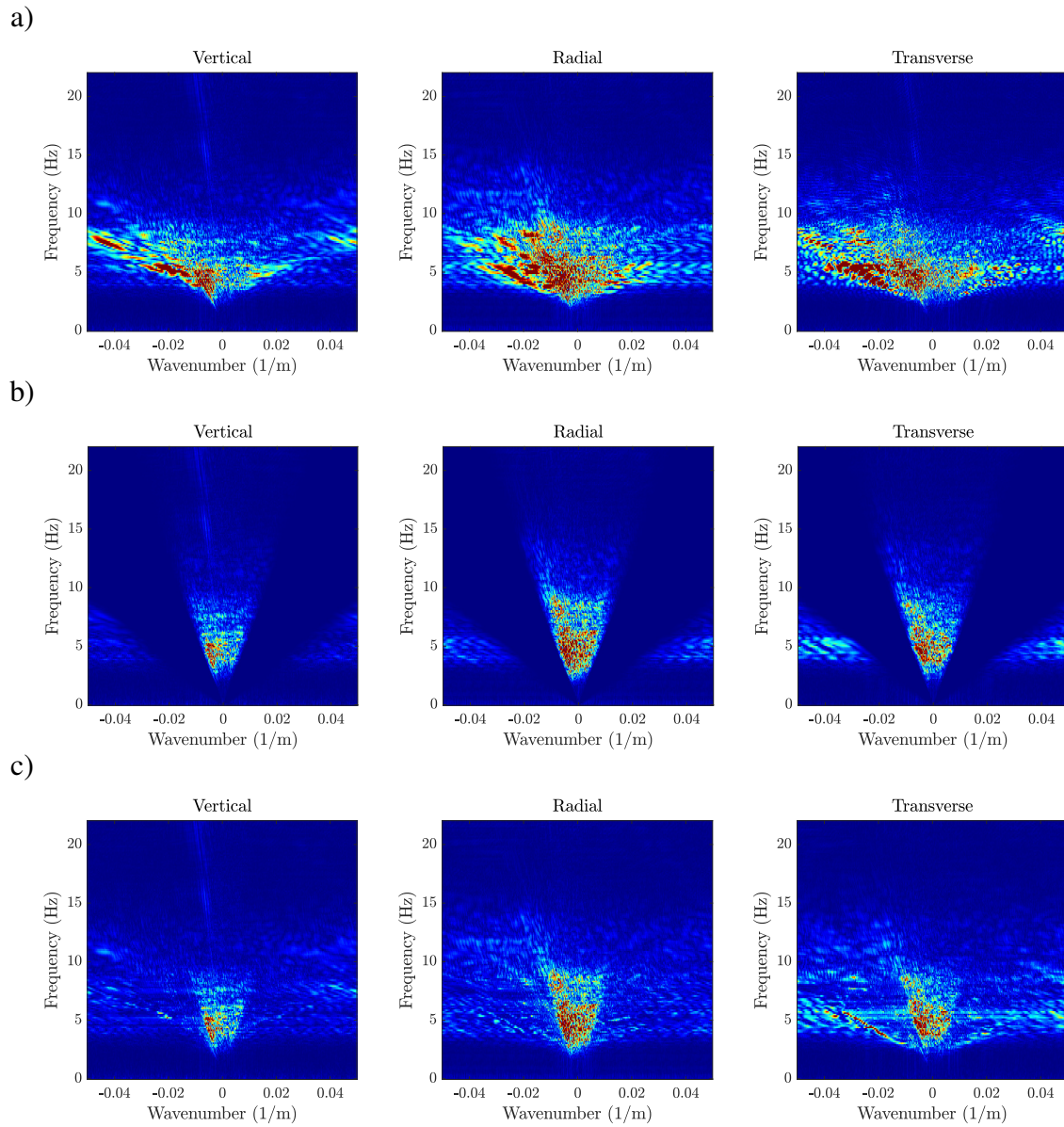


FIG. 6.  $f - k$  spectra of seismic data for (a) raw data, (b) data after  $f - k$  filter, and (c) data after 3CPR filter

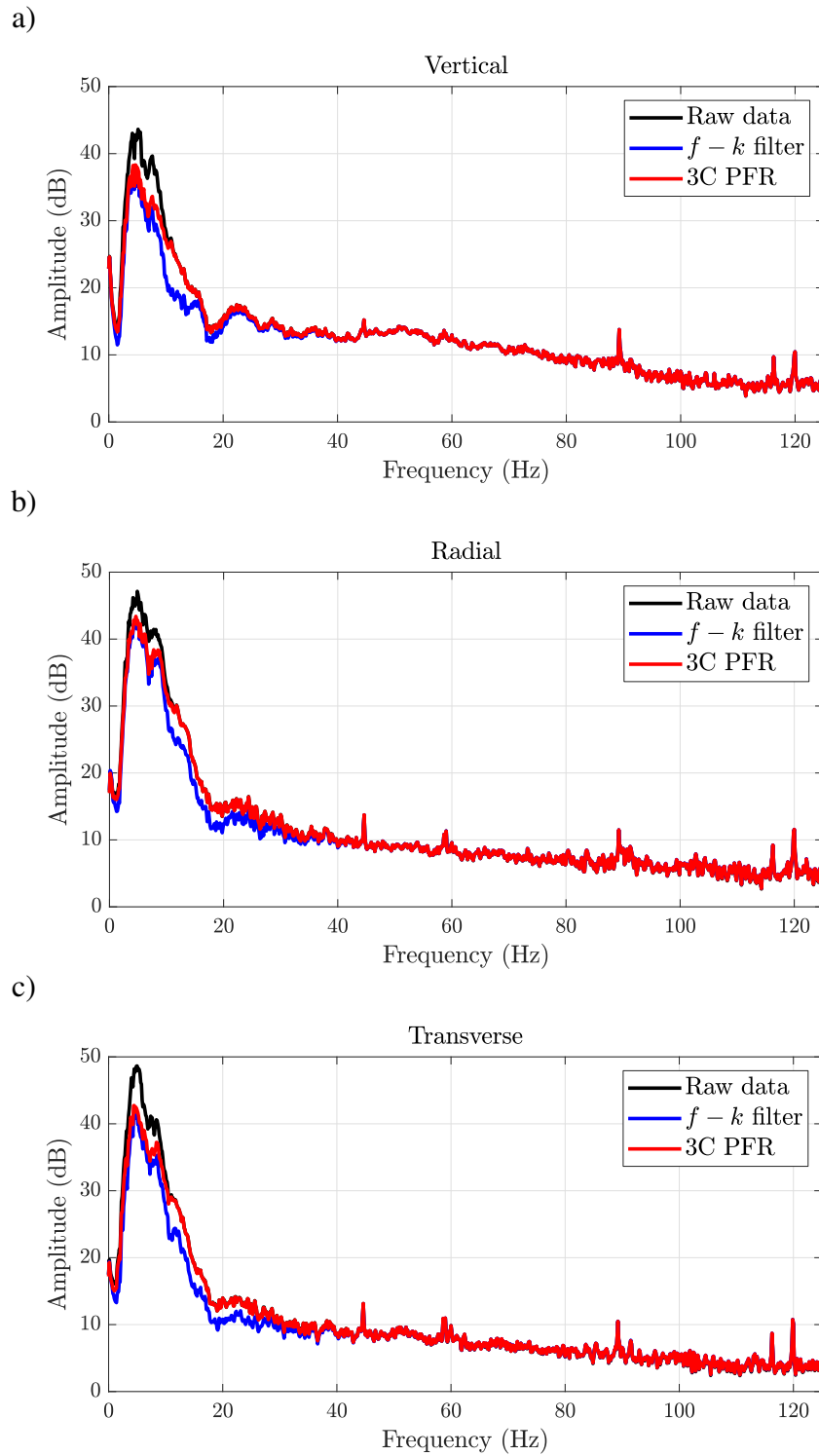


FIG. 7. Spectra of seismic data of raw data (black), filtered data with  $f - k$  filter (blue), and 3C polarization filter based in Radon transform (red). (a) Vertical component, (b) Radial component , and (c) Transverse component.